Oxidation of Antibacterial Molecules by Aqueous Ozone: Moiety-Specific Reaction Kinetics and Application to Ozone-Based Wastewater Treatment

MICHAEL C. DODD,
MARC-OLIVIER BUFFLE, AND
URS VON GUNTEN*

*Swiss Federal Institute of Aquatic Science and Technology
(EAWAG), Duebendorf, Switzerland CH-8600*

Ozone and hydroxyl radical (•OH) reaction kinetics were measured for 14 antibacterial compounds from nine structural families, to determine whether municipal wastewater ozonation is likely to result in selective oxidation of these compounds' biochemically essential moieties. Each substrate is oxidized by ozone with an apparent second-order rate constant, $k'_{O_3,app} > 1 \times 10^3$ M^{-1} s^{-1}, at pH 7, with the exception of $N(4)$-acetylsulfamethoxazole ($k'_{O_3,app}$ is 2.5×10^2 M^{-1} s^{-1}). $k'_{O_3,app}$ values (pH 7) for macrolides, sulfamethoxazole, trimethoprim, tetracycline, vancomycin, and amikacin appear to correspond directly to oxidation of biochemically essential moieties. Initial reactions of ozone with $N(4)$-acetylsulfamethoxazole, fluoroquinolones, lincomycin, and β-lactams do not lead to appreciable oxidation of biochemically essential moieties. However, ozone oxidizes these moieties within fluoroquinolones and lincomycin via slower reactions. Measured $k'_{O_3,app}$ values and second-order •OH rate constants, $k''_{•OH,app}$, were utilized to characterize pollutant losses during ozonation of secondary municipal wastewater effluent. These losses were dependent on $k'_{O_3,app}$, but independent of $k''_{•OH,app}$. Ozone doses ≥ 3 mg/L yielded $\geq 99\%$ depletion of fast-reacting substrates ($k'_{O_3,app} > 5 \times 10^4$ M^{-1} s^{-1}) at pH 7.7. Ten substrates reacted predominantly with ozone; only four were oxidized predominantly by •OH. These results indicate that many antibacterial compounds will be oxidized in wastewater via moiety-specific reactions with ozone.

Introduction

Clinically important antibacterial agents are virtually ubiquitous contaminants of municipal wastewaters (Supporting Information, Figure S1) (*1−5*). Raw and primary wastewaters typically contain compounds from various antibacterial classes at individual concentrations ranging from 0.5 to 3 μg/L (Figure S1). These concentrations can often be reduced by 60−90% during conventional activated sludge treatment combined with tertiary filtration (*2, 4, 6*). This is generally sufficient to achieve effluent concentrations below levels known to be detrimental to bacteria (Figure S1) and other aquatic life (*7, 8*). However, effluent concentrations of certain antibacterials (e.g., fluoroquinolones (*2, 3*)) may still be harmful to organisms present in effluent-dominated receiving

waters (*9*). In addition, because activated sludge processes typically operate at solids retention times of several days, conventional wastewater treatment results in prolonged exposure of *wastewater-borne* bacteria to significantly higher antibacterial concentrations than are present in treated effluents (*2, 4−6*). In the case of fluoroquinolones, these concentrations can approach minimal growth inhibitory concentrations (MICs) for *E. coli* (Figure S1) and other bacterial strains (*10*)—a condition that may favor evolution of low-level antibacterial resistance in affected bacterial communities (*11, 12*).

In the interest of precaution, unnecessary exposure of wastewater-borne and environmental microbiota to biochemical stress originating from antibacterial compounds should be minimized when possible. Supplemental wastewater treatment technologies capable of yielding rapid biochemical deactivation of such compounds could aid in achieving this objective. Ozonation, which is utilized in advanced treatment of secondary wastewater effluent (*13*), and has shown potential as a means of preoxidizing and disinfecting primary wastewater effluents (*14, 15*), appears promising in this regard (*16−18*). Recent studies have shown that relatively low ozone (O₃) doses (≤ 5 mg/L) can yield $>90\%$ depletion of many antibacterial compounds in wastewaters containing DOC concentrations as high as 23 mg C/L (*18, 19*). Although mineralization of antibacterial molecules will be infeasible during municipal wastewater ozonation, partial oxidation may be sufficient to achieve their biochemical deactivation, provided that O₃ reacts with the parent molecules in a manner leading to rapid, selective oxidation of functional moieties related to their antibacterial activities. Such an outcome has been demonstrated for the steroid hormone 17α-ethinylestradiol, in which case ozone selectively oxidizes the phenol moiety responsible for the parent molecule's estrogenic activity (*20*). Similar results appear likely for many antibacterial molecules (Table 1, Text S1). However, some antibacterial compounds' biochemically essential moieties may be O₃-refractory, or O₃ may react preferentially with moieties nonessential to the parent molecules' biochemical activities (Table 1). In such cases, relative reactivities of *essential* and *nonessential* functional moieties will influence the likelihood that antibacterial compounds can be biochemically deactivated during wastewater ozonation.

pH-dependent variations in measured *apparent* rate constants can be used to determine *specific* rate constants for reactions of O₃ with each individual acid−base species of an ionizable substrate (*21−23*). This approach was applied in the present study to evaluate O₃ reaction kinetics measured for 14 antibacterial molecules representing nine of the most widely used antibacterial structural families (Table 1). O₃ reaction kinetics for substructure model substrates (Table 2) representing the theorized reactive moieties within each antibacterial molecule were measured to facilitate assignment of calculated species-specific reactivities to individual functional moieties.

Pollutant transformation during wastewater ozonation is also influenced by hydroxyl radicals (•OH) generated through reactions of O₃ with specific functional moieties in dissolved organic matter (*24, 25*) or from autocatalytic O₃ decomposition (*26*). Because •OH reacts rapidly with a wider variety of functional moieties than O₃, the oxidative specificity of an ozonation process may be diminished if dominated by •OH reactions. The importance of •OH and O₃ in the context of antibacterial compound oxidation was investigated by using rate constants determined here to characterize observed

* Corresponding author phone: +41 44 823 52 70; fax: +41 44 823 52 10; e-mail: vongunten@eawag.ch.

10.1021/es051369x CCC: $33.50   © 2006 American Chemical Society
Published on Web 02/07/2006

VOL. 40, NO. 6, 2006 / ENVIRONMENTAL SCIENCE & TECHNOLOGY ■ **1969**

TABLE 1. Antibacterial Substrates and Expected Sites of O₃ Attack^{a-d}

Macrolides

Roxithromycin (RX)
$pK_a = 9.2$

Azithromycin (AZ)
$pK_{a1,2} = 8.7, 9.5$

Tylosin (TYL)
$pK_a = 7.7$

Sulfonamides — **DHFR Inhibitor^e**

Sulfamethoxazole (SMX)
$pK_{a1,2} = 1.7, 5.6$

N(4)-acetyl-sulfamethoxazole (ASMX)
$pK_a = 5.5$

Trimethoprim (TMP)
$pK_{a1,2} = 3.2, 7.1$

Fluoroquinolones — **Lincosamide**

Ciprofloxacin (CF)
$pK_{a1,2} = 6.2, 8.8$

Enrofloxacin (EF)
$pK_{a1,2} = 6.1, 7.7$

Lincomycin (LM)
$pK_a = 7.8$

β-lactams — **Tetracycline**

Penicillin G (PG)
$pK_a = 2.7$

Cephalexin (CP)
$pK_{a1,2} = 2.5, 7.1$

Tetracycline (TET)
$pK_{a1,2,3} = 3.3, 7.7, 9.7$
*pK_{a1} and pK_{a3} are group values

Glycopeptide — **Aminoglycoside**

Amikacin (AM)
$pK_{a1,2,3,4} = 6.7, 8.4, 8.4, 9.7$

Vancomycin (VM)
$pK_{a1,2,3,4,5,6} = 2.9, 7.2, 8.6, 9.6, 10.5, 11.7$

^{a} Structural families are listed in bold. ^{b} O₃ target sites classified as *essential* (i.e., these moieties are directly responsible for the parent molecules' antibacterial activities; see Text S1) are indicated by solid arrows. O₃ target sites classified as *nonessential* (i.e., these moieties are not directly responsible for the parent molecules' antibacterial activities) are indicated by dotted arrows. ^{c} References from which pK_a values were obtained are summarized in the Supporting Information, Table S1. ^{d} Sites of ionization are numbered according to order of deprotonation. For compounds possessing a single pK_a, the ionizable site is labeled "1". ^{e} DHFR, dihydrofolate reductase.

antibacterial compound losses during ozonation of a secondary wastewater effluent.

Materials and Methods

Chemical Reagents. All reagents were of 95% purity or greater, with the exception of ASMX, which was ~70% pure. Descriptions of chemical sources and stock solutions are provided in the Supporting Information, Text S2.

Measurement of Rate Constants. O₃ and •OH rate constant measurements were conducted according to seven experimental protocols (designated I–VII), which are summarized in Table 3 and described in detail within Text S3. Solution pH was maintained in all kinetic experiments with phosphate buffers of approximately 10 mM concentration. *t*-BuOH (10 mM) was added as a •OH scavenger to solutions used for measurement of O₃ rate constants. O₃ and •OH rate constants were measured at 20 (±0.5) °C (in accordance with previously determined O₃ reaction kinetics (*17, 21, 27, 28*)) and 25 (±0.5) °C, respectively.

Wastewater Matrix Experiments. Wastewater experiments were conducted in batch, by monitoring losses of each substrate in a sample of Kloten-Opfikon secondary waste-water effluent for various O₃ doses, at 20 (±0.5) °C (see Text S4 for experimental details). Sample pH, alkalinity, and DOC were 7.7, 3.5 mM as HCO₃⁻, and 5.3 mg of C/L, respectively.
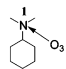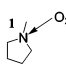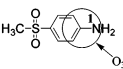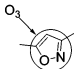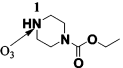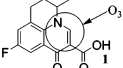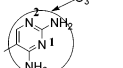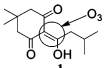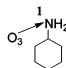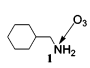
Results and Discussion

Moiety-Specific Ozone Reaction Kinetics. pH-dependent, apparent second-order rate constants, $k''_{O_3,app}$, were determined for each substrate at pH values ranging from 3 to 9, according to the methods described within the Supporting Information (Text S3). pH dependencies of measured $k''_{O_3,app}$ values were modeled according to a modified second-order rate expression (eq 1) that incorporates acid–base speciation of substrate, M:

$$\frac{d[M]_T}{dt} = \frac{1}{\eta}\frac{d[O_3]}{dt} = -k''_{O_3,app,M}[O_3][M]_T = -\sum_{i=1}^{n} k''_i [O_3]\alpha_i [M]_T \tag{1}$$

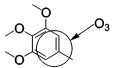where $[M]_T$ represents the total concentration of M (including all n acid–base species), η represents an apparent stoichiometric factor accounting for moles of O₃ consumed per mole of substrate consumed, k''_i is the specific rate constant

TABLE 2. Substructure Model Substrates and Expected Sites of O$_3$ Attack[a,b]

N,N-dimethylcyclo-hexylamine (DMCH) pK_a = 10.7 Model for: RX, AZ, TYL, TET	1-methylpyrrolidine (MP) pK_a = 10.2 Model for: AZ, LM	4-aminophenyl methyl sulfone (APMS) pK_a = 1.5 Model for: SMX	3,5-dimethylisoxazole (DMI) Model for: SMX, ASMX
Ethyl N-piperazine-carboxylate (EPC) pK_a = 8.3 Model for: CF, EF	Flumequine (FLU) pK_a = 6.5 Model for: CF, EF	2,4-diamino-5-methylpyrimidine (DAMP) p$K_{a1,2}$ = 3.2, 7.1 Model for. TMP	3,4,5-trimethoxytoluene (TMT) Model for: TMP, VM
2-(3-methylbutyryl)-5,5-dimethyl-1,3-cyclohexandione (MBDCH) pK_a = 3.5 Model for: TET	Cyclohexylamine (CH) pK_a = 10.6 Model for: AM	Cyclohexane-methylamine (CHM) pK_a = 10.3 Model for: AM	

[a] References from which pK_a values were obtained are summarized in the Supporting Information, Table S2. [b] In the case of DAMP, which has two pK_a's, sites of ionization are numbered according to order of deprotonation. Sites of ionization are labeled "1" for all other ionizable compounds.

TABLE 3. Experimental Methods Used for Rate Constant Measurements (Details in Text S3)

method	oxidant	experimental procedure[a]	measurement endpoint
I	O$_3$	SFL	O$_3$ loss (measured at λ = 258 nm)
II	O$_3$	Batch	substrate loss (measured by HPLC)
III	O$_3$	CK	reaction product yields (measured by various techniques[b])
IV	O$_3$	CK	losses of each competitor (measured by HPLC)
V	•OH	CK (H$_2$O$_2$ photolysis)	losses of each competitor (measured by HPLC)
VI	•OH	CK (γ-radiolysis)	losses of each competitor (measured by HPLC)
VII	•OH	CK (H$_2$O$_2$ photolysis, amine derivatization)	losses of each competitor (measured by HPLC)

[a] SFL, stopped-flow spectrophotometry; CK, competition kinetics. [b] Reaction products were measured either spectrophotometrically or by HPLC, depending on the analyte.

corresponding to reaction of O$_3$ with substrate acid−base species i, and α_i represents the equilibrium distribution coefficients for species i. k_i'' values—summarized in Table 4 and Table S3—were calculated by nonlinear regression of experimental data according to eq 2

$$k_{O_3,app,M}'' = \sum_{i=1}^{n} k_i'' \alpha_i \tag{2}$$

via a Marquardt−Levenberg curve-fitting routine (SigmaPlot 2002, SPSS software).

Macrolides. *Roxithromycin (RX).* The strong pH dependency of $k_{O_3,app,RX}''$ (Figure 1a) indicates that O$_3$ reacts initially at the RX structure's neutral tertiary amine moiety (Table 1) (17). The continuous decrease in $k_{O_3,app,RX}''$ with decreasing pH—due to protonation of RX's tertiary amine (17, 21, 22)—suggests that O$_3$ reactivity with the remainder of the RX structure is very low, and that oxidation at circumneutral pH will occur exclusively at the deprotonated tertiary amine. The pH dependency and magnitudes of $k_{O_3,app}''$ measured for N,N-dimethylcyclohexylamine (DMCH, Table 2) (Figure 1a) support these conclusions.

Azithromycin (AZ). $k_{O_3,app,AZ}''$ exhibits nearly the same pH dependency as $k_{O_3,app,RX}''$ (Figure 1a). However, the close proximity of pK_{a1} and pK_{a2} values for AZ prevents one from determining whether $k_{O_3,app,AZ}''$ is due primarily to reaction of O$_3$ with the parent molecule's exocyclic tertiary amine or with its heterocyclic tertiary amine (Table 1). Comparison of the rate constant for reaction of neutral 1-methylpyrrolidine (MP in Table 2) with O$_3$ to that for neutral DMCH shows that the two values are quite similar (Figure 1a). This suggests that the corresponding moieties in the AZ structure (Table 1) react with O$_3$ at roughly equivalent rates.

Tylosin (TYL). TYL reacts with O$_3$ significantly faster than RX and AZ at acidic pH (Figure 1a). This can be attributed primarily to the conjugated diene moiety within TYL's macrolactone ring (Table 1). Olefins typically react with O$_3$ at rates that are independent of pH, within the range 10^5–10^6 M^{-1} s^{-1}, unless substituted with strong electron-withdrawing groups (27, 31). The rate constant reported for the neutral form of the model diene sorbic acid (k_{O_3}'' = 3.2 × 10^5 M^{-1} s^{-1} (32)) is within a factor of ~4 of that for the TYL cation (Figure 1a). This provides additional evidence that the diene moiety is responsible for TYL's high reactivity toward O$_3$ under acidic conditions. At pH >6, the proportion of neutral TYL (i.e.,

TABLE 4. Second-Order Rate Constants (M⁻¹ s⁻¹) for Reactions of Antibacterial Substrates with O_3 and •OH[a]

substrate[b] (rate const. meas. methods[c])	k''_{O_3}[d] diprotonated species	monoprotonated species	deprotonated species	$k''_{O_3,app}$[d] (pH 7)	$k''_{O_3,app}$[d] (pH 7.7)	$k''_{•OH,app}$[e] (pH 7)
RX (I, V)	NA[f]	<1 (17)[g]	$1.0\ (\pm0.1) \times 10^7$ (17)[k]	6.3×10^4	3.1×10^5	$5.4\ (\pm0.3) \times 10^9$
AZ (I, V)	<1[g]	$6.0\ (\pm1.1) \times 10^6$	$6.0\ (\pm21.9) \times 10^6$ [l]	1.1×10^5	5.2×10^5	$2.9\ (\pm0.6) \times 10^9$
TYL (IV, VI)	NA[f]	$7.7\ (\pm1.4) \times 10^4$	$2.7\ (\pm0.5) \times 10^6$	5.1×10^5	1.4×10^6	$8.2\ (\pm0.1) \times 10^9$
SMX (IV)	ND[f]	$4.7\ (\pm0.9) \times 10^4$	$5.7\ (\pm1.0) \times 10^5$	5.5×10^5	5.7×10^5	$5.5\ (\pm0.7) \times 10^9$ (17)
ASMX (II, V)	NA[f]	$2.0\ (\pm0.2) \times 10^1$	$2.6\ (\pm0.1) \times 10^2$	2.5×10^2	2.6×10^2	$6.8\ (\pm0.1) \times 10^9$
CF (II, IV, VI)	$4.0\ (\pm1.2) \times 10^2$	$7.5\ (\pm2.8) \times 10^3$ [i]	$9.0\ (\pm3.1) \times 10^5$	1.9×10^4	7.1×10^4	$4.1\ (\pm0.3) \times 10^9$
EF (II, IV, VI)	$3.3\ (\pm1.3) \times 10^2$	$4.6\ (\pm1.2) \times 10^4$ [i]	$7.8\ (\pm1.9) \times 10^5$	1.5×10^5	4.1×10^5	$4.5\ (\pm0.4) \times 10^9$
TMP (IV, V)	$3.3\ (\pm3.0) \times 10^4$	$7.4\ (\pm1.8) \times 10^4$	$5.2\ (\pm1.0) \times 10^5$	2.7×10^5	4.3×10^5	$6.9\ (\pm0.2) \times 10^9$
LM (V)	NA[f]	$3.3\ (\pm0.1) \times 10^5$ (23)	$2.8\ (\pm0.1) \times 10^6$ (23)	6.7×10^5	1.4×10^6	$8.5\ (\pm0.2) \times 10^9$
PG (II, V)	NA[f]	$4.8\ (\pm0.1) \times 10^3$ [j]	$4.8\ (\pm0.1) \times 10^3$ [j]	4.8×10^3	4.8×10^3	$7.3\ (\pm0.3) \times 10^9$ [m]
CP (III, V)	ND[f]	$8.2\ (\pm2.9) \times 10^4$	$9.3\ (\pm2.2) \times 10^4$	8.7×10^4	9.1×10^4	$8.5\ (\pm0.7) \times 10^9$
TET (III, VI)	$9.4\ (\pm0.6) \times 10^4 - 4.7\ (\pm0.3)\ 10^6$ (pH 3−9; see Figure 2)[h]			1.9×10^6	3.2×10^6	$7.7\ (\pm1.2) \times 10^9$
VM (IV, V)	$1.1\ (\pm0.1) \times 10^4 - 9.1\ (\pm1.1)\ 10^5$ (pH 3−8; see Figure 2)[h]			6.1×10^5	8.1×10^5	$8.1\ (\pm0.3) \times 10^9$
AM (I, VII)	$1.3\ (\pm0.7) \times 10^1 - 1.1\ (\pm0.2) \times 10^4$ (pH 4.1 to 8.9; see Figure 2)[h]			1.8×10^3	4.9×10^3	$7.2\ (\pm0.3) \times 10^9$

[a] Values obtained from the current investigation, unless indicated otherwise. [b] For full names, see Table 1. [c] Described in Table 3. For CF, II was used from pH 3−6, and IV from pH 6.5−8. For EF, II was used from pH 3−5.5, and IV from pH 6−8. [d] 20(±0.5) °C. [e] 25(±0.5) °C. [f] NA, not applicable; ND, not determined. [g] Protonated amine reactivity assumed to be negligible, on the basis of prior observations (21, 22). [h] Only ranges of $k''_{O_3,app}$ are listed for these compounds. [i] k''_{O_3} for the "monoprotonated" fluoroquinolone species represents an "effective" rate constant for the combination of zwitterionic and neutral species. [j] PG reactivity is assumed to be independent of acid-base speciation, because its dissociable functional groups are not conjugated with its thioether (Table 1). [k] Rate constant recalculated with $pK_{a,RX} = 9.2$, using data reported by Huber et al. (17). [l] The small difference between AZ's pK_{a1} and pK_{a2}—combined with lack of data at pH >6.8—prevented accurate determination of k''_{O_3} for neutral AZ. [m] This value agrees well with that reported by Phillips et al. (29), corrected according to Neta and Dorfman (1968) (30) (i.e., $k''_{•OH,app,PG} = 7.1 \times 10^9$ M⁻¹ s⁻¹ at pH 7).

deprotonated tertiary amine) becomes high enough to influence the magnitude of $k''_{O_3,app,TYL}$, and dominates measured reactivities for more alkaline pH ranges (Figure 1a).

Sulfonamides. *Sulfamethoxazole (SMX).* The apparent rate constants measured for reaction of SMX with O_3 range from ~5×10^4 to ~5×10^5 M⁻¹ s⁻¹ between pH 3 and 7 (Figure 1b). The specific rate constant calculated for the SMX anion (Table 4) agrees within a factor of 2.2 with that previously determined by Huber et al. (17), after correction for the different O_3 consumption stoichiometries of the reference competitor substrates—cinnamic acid (28) and phenol (24, 33)—used in the current and former studies. Neutral 4-aminophenyl methyl sulfone (APMS in Table 2)—which approximates SMX's aniline moiety—reacts with O_3 with the same rate constant calculated for the neutral SMX species (Table 4, Figure 1b). In contrast, 3,5-dimethylisoxazole (DMI in Table 2)—a model for SMX's isoxazole group—reacts very slowly with O_3 (Figure 1b). These results indicate that reaction of O_3 with the SMX structure takes place primarily at the biochemically active *p*-sulfonylaniline moiety. The pH dependency of $k''_{O_3,app,SMX}$ (Figure 1b) appears to correlate with deprotonation of SMX's sulfonamide nitrogen (Table 1). However, rapid reaction between O_3 and the sulfonamide nitrogen can be ruled out (21, 22). Therefore, this effect seems to be due to activation of the SMX molecule's aniline moiety (Table 1) toward electrophilic attack by O_3, via deprotonation of the sulfonamide nitrogen.

N(4)-Acetylsulfamethoxazole (ASMX). A high percentage of SMX enters wastewater treatment facilities as the metabolite ASMX (Table 1)—which can be retransformed to SMX during biological treatment (4). The rate constants determined for reaction of ozone with ASMX's neutral and anionic species are 20 and 2.6×10^2 M⁻¹ s⁻¹, respectively, more than 3 orders of magnitude lower than for SMX (Figure 1b). These results agree with prior observations that ASMX is poorly degraded during ozonation of secondary wastewater effluent (18). The decrease in reactivity from anionic ASMX to neutral ASMX (Table 4, Figure 1b) likely reflects enhancement of the sulfonamide moiety's electron-withdrawing strength upon sulfonamide nitrogen protonation. Because this effect should reduce the O_3 reactivities of both the ASMX isoxazole ring

and the *p*-sulfonylaniline ring, it is unclear which moiety dominates observed reaction kinetics (Figure 1b).

Fluoroquinolones. *Ciprofloxacin (CF).* CF's reactivity toward O_3 is strongly dependent on pH, where $k''_{O_3,app,CF}$ ranges from ~4×10^2 to more than 10^5 M⁻¹ s⁻¹ between pH 3 and 8 (Figure 1b). The pH dependency of $k''_{O_3,app,CF}$ indicates that this trend is governed by deprotonation of CF's N(4) amine (Table 1). This hypothesis is supported by the reactivity of O_3 with ethyl *N*-piperazinecarboxylate (EPC in Table 2). $k''_{O_3,app,EPC}$ exhibits nearly the same pH dependency and magnitudes as $k''_{O_3,app,CF}$ between pH 5 and 8 (Figure 1b). Flumequine (FLU in Table 2)—a surrogate for the biochemically active quinolone moiety (Table 1)—also exhibits pH-dependent reaction kinetics. However, values of $k''_{O_3,app,FLU}$ are several orders of magnitude lower than those observed for CF's N(4) amine (Figure 1b). The baseline reactivity observed for the CF molecule at pH <4 (Figure 1b) cannot be attributed to reactions with the N(4) atom or the quinolone heterocyclic ring (Figure 1b). This reactivity must therefore be due to reactions taking place either at the piperazine N(1) atom or at the unsubstituted ortho position of the adjacent aromatic ring.

Enrofloxacin (EF). EF reacts with O_3 at higher rates than CF in the pH region between 3 and 8 (Figure 1b). This effect is due primarily to the difference in CF's and EF's pK_{a2} values (Table 1). At pH 7, for example, the molar fraction of anionic CF (in which the N(4) amine is deprotonated) is 0.01, compared to 0.15 for EF. However, the apparent rate constants for CF and EF converge at higher pH (Figure 1b), indicating a close similarity in the absolute reactivities of their N(4) atoms.

Trimethoprim (TMP). Measured magnitudes of $k''_{O_3,app,TMP}$ range from high-10^4 to mid-10^5 M⁻¹ s⁻¹ (Figure 1c). The observed variation in $k''_{O_3,app,TMP}$ (Figure 1c) can most likely be attributed to speciation of TMP's diaminopyrimidine moiety (Table 1). Protonation at the heterocyclic N(1) and N(3) nitrogens (Table 1) should reduce this moiety's O_3 reactivity via coordination of the resonant lone-pair electrons associated with each of TMP's two exocyclic amines. 2,4-Diamino-5-methylpyrimidine (DAMP in Table 2) also exhibits pH-dependent variation in its apparent O_3 reaction rate
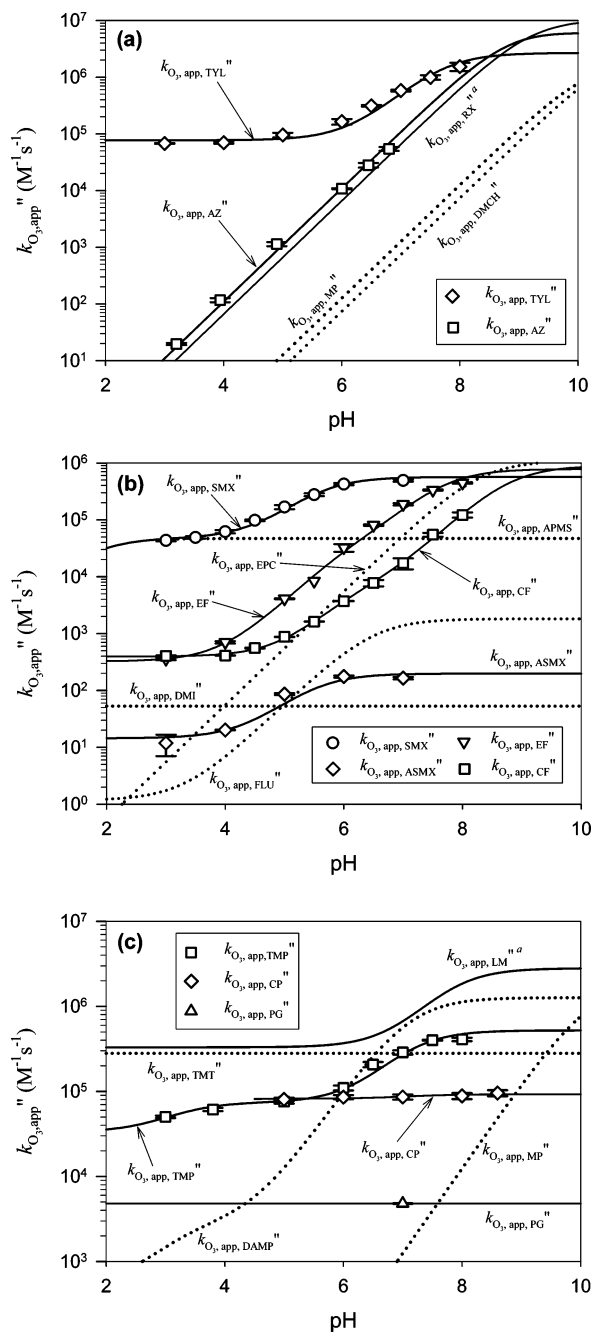
FIGURE 1. Apparent second-order rate constants for reactions of parent substrates and associated substructure model substrates with O_3 at 20 (± 0.5) °C (symbols = measurements; lines = model predictions): (a) macrolides (RX, AZ, and TYL) with associated substructure models; (b) sulfonamides (SMX and ASMX) and fluoroquinolones (CF and EF) with associated substructure models; (c) TMP, LM, and β-lactams (PG and CP) with associated substructure models. [a] $k''_{O_3,app,RX}$ and $k''_{O_3,app,LM}$ were calculated from data reported by Huber et al. (17) and Qiang et al. (23), respectively.

constant (Figure 1c). However, the specific rate constants calculated for mono- and diprotonated DAMP (Table S3) are substantially lower than those calculated for the corresponding TMP species (Table 4, Figure 1c). The high O_3 reactivity of 3,4,5-trimethoxytoluene (TMT in Table 2)—a surrogate for TMP's trimethoxytolyl moiety (Table 1)—suggests that the trimethoxytolyl moiety accounts for the high reactivity of the protonated TMP species (Figure 1c). The difference in reactivities of TMT and TMP's protonated species could be a consequence of the TMP diaminopyrim-

idine moiety's bulk, which may hinder attack by O_3 at the 2- and 6-positions of the TMP structure's trimethoxytolyl moiety (Table 1).

Lincomycin (LM). $k''_{O_3,app,LM}$ is constant below pH 5 and increases above pH 5 to a calculated maximum of 2.8×10^6 M^{-1} s^{-1} (Figure 1c) (23). LM's baseline reactivity can be attributed to pH-independent kinetics of the reaction between its thioether and O_3, since its heterocyclic amine is protonated—and essentially unreactive toward O_3—under these conditions (23). Likewise, the variation in $k''_{O_3,app,LM}$ above pH 5 can be attributed to reaction of O_3 with the neutral heterocyclic amine (23). $k''_{O_3,app}$ values measured for MP—a model for LM's heterocyclic tertiary amine (Table 1)—are consistent with these conclusions (Figure 1c).

β-Lactams. *Penicillin G (PG).* PG possesses only one functional moiety—a thioether (Table 1)—that can be expected to account for its observed reactivity toward O_3 (Figure 1c). Reaction kinetics for this moiety are expected to be independent of pH (22, 23).

Cephalexin (CP). $k''_{O_3,app,CP}$ is a little more than 1 order of magnitude higher than $k''_{O_3,app,PG}$ on average (Figure 1c). The relatively high magnitude of $k''_{O_3,app,CP}$ at pH <7 suggests that reactivity of CP at acidic pH is attributable to oxidation of its double bond or thioether (Table 1), each of which is expected to exhibit pH-independent O_3 reaction kinetics. However, the slight increase in $k''_{O_3,app,CP}$ above pH 7 (Figure 1c) suggests that the primary amine ($pK_a = 7.1$, Table 1) may govern CP reactivity at circumneutral and higher pH values.

Substrates with More Than Two pK_a Values. The complexity of TET's, VM's, and AM's speciation patterns precluded accurate modeling of O_3 reaction kinetics by the approaches utilized above. However, $k''_{O_3,app,TET}$, $k''_{O_3,app,VM}$, and $k''_{O_3,app,AM}$ were compared to substructure model substrate data (Figure 2) to facilitate preliminary assignment of moiety-specific O_3 reaction kinetics.

TET reacts rapidly with O_3 over a wide range of pHs (Figure 2). Because the rate of reaction with the tertiary amine ($pK_a = 7.7$, Table 1) is not likely to be appreciable relative to the remainder of the TET molecule below pH 5 (Figure 2), the TET structure's observed reactivity toward O_3 at acidic pH is likely due to oxidation of the tetracycline ring system. Although tertiary amine reactivity could be important above pH 7, the high reactivity of various phenolic structures (21, 24) and 2-(3-methylbutyryl)-5,5-dimethyl-1,3-cyclohexan-dione (MBDCH in Table 2)—a surrogate for the olefinic bonds within TET's tetracyclic ring system (Table 1)—indicate that O_3 reacts primarily with the ring system at circumneutral pH, as well.
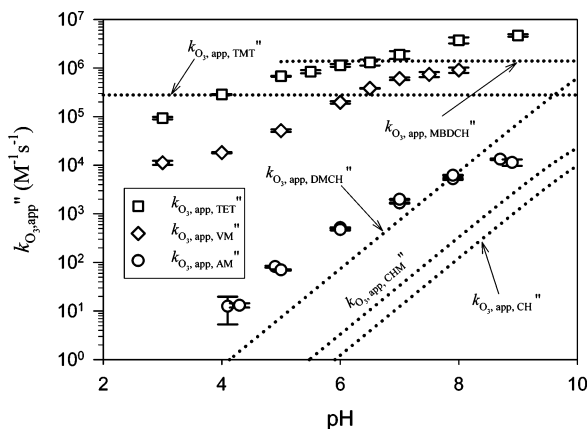

FIGURE 2. Apparent second-order rate constants for reactions of TET, VM, AM, and associated substructure models with O_3 at 20 (± 0.5) °C (symbols = measurements; lines = model predictions).
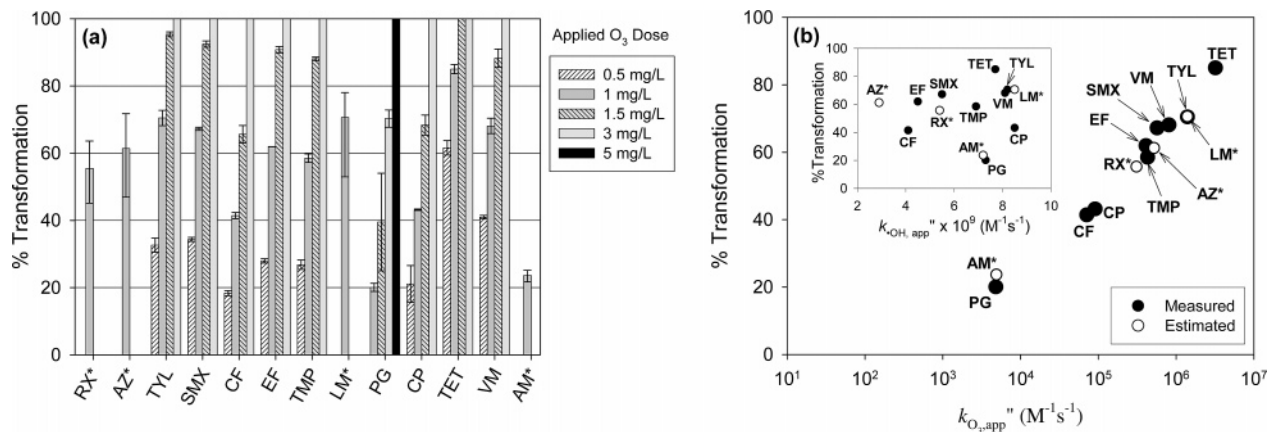
FIGURE 3. Antibacterial substrate transformation during ozonation of Kloten-Opfikon wastewater at 20 ($\pm$0.5) °C, pH 7.7, and [substrate]$_0$ = 1 μM. (a) Measured transformation efficiencies at varying O$_3$ dosages, for substrates with $k''_{O_3,app} > 10^3$ M^{-1} s^{-1}. (b) Dependence of transformation efficiencies on $k''_{O_3,app}$, at an O$_3$ dose of 1 mg/L (21 μM). Inset shows independence of transformation efficiency from $k''_{•OH,app}$. The asterisks (*) indicate that % transformation values for RX, AZ, LM, and AM were estimated via procedures described in Text S5.

VM is also highly reactive toward O$_3$ between pH 3 and 8 (Figure 2). The high measured reactivity of TMT (Table 2, Figure 2), a surrogate for VM's trimethoxybenzyl moiety, in addition to the high known reactivity of phenols and resorcinols toward O$_3$ at all pH conditions (*21*, *24*), suggests that $k''_{O_3,app,VM}$ at pH <7 corresponds to oxidation of the biochemically essential aromatic target sites shown in Table 1, since oxidation of VM's amine moieties should not be important at acidic pH. However, the *N*-methylleucine moiety may react rapidly enough with O$_3$ to influence observed reaction kinetics at pH >7, on the basis of known secondary amine reaction kinetics (*21*, *22*).

$k''_{O_3,app,AM}$ varies from roughly 10 to just over 10^4 M^{-1} s^{-1} between pH 4 and 9 (Figure 2). The measured pH dependency of $k''_{O_3,app,AM}$ is consistent with oxidation of AM's primary amine moieties (with pK_a values ranging from 6.7 to 9.7, Table 1). In addition, $k''_{O_3,app,AM}$ near pH 9 (at which all but one of AM's amines are predominantly deprotonated) is within an order of magnitude of k''_{O_3} for neutral butylamine (1.2 × 10^5 (*22*)), cyclohexanemethylamine (CHM in Table 2, with 7.1 × 10^4, from Table S3), and cyclohexylamine (CH in Table 2, with 4.9 × 10^4 M^{-1} s^{-1}, from Table S3)—which can be taken as structural approximations of AM's primary amine groups (Table 1).

Moiety-Specific Oxidation vs Parent Molecule Disappearance. The preceding discussion indicates that initial reactions of O$_3$ with many parent antibacterial substrates occur at biochemically essential target moieties (Table 1). Consequently, $t_{1/2}$ values for observed transformations of many parent molecules correspond to $t_{1/2}$ for their essential target moieties (Figure S11). However, $t_{1/2}$ for reaction of O$_3$ with FLU—which approximates CF's and EF's biochemically essential quinolone moieties—is 14 times longer at pH 7 than $t_{1/2,CF}$ (which corresponds to oxidation of the nonessential piperazine moiety) and 109 times longer than $t_{1/2,EF}$ (Figure S11), indicating that observed losses of parent fluoroquinolones during ozonation may not necessarily correspond directly to elimination of their antibacterial activities. In addition, O$_3$ does not appear to oxidize essential targets in the ASMX, PG, or CP molecules at appreciable rates. However, the O$_3$ recalcitrance of the latter three compounds' essential target moieties may be of relatively minor importance, since prior findings indicate that ASMX and β-lactams in general are unlikely to be discharged to surface waters at significant concentrations (*1*, *4*).

Studies in Wastewater Matrixes. *Depletion of Parent Molecules.* Oxidation of 1 μM ASMX—the substrate reacting slowest with O$_3$ (Table 4)—was monitored in batch experi-

ments with Kloten-Opfikon wastewater at an O$_3$ dose of 63 μM (3 mg/L) (Figure S12). Approximately 35% of [ASMX]$_0$ remained after nearly complete depletion of O$_3$. The observed recalcitrance of ASMX is consistent with observations for pilot-scale ozonation of Kloten-Opfikon secondary effluent (*18*).

Significant residuals of PG also remained at an O$_3$ dose of 3 mg/L (63 μM) (Figure 3a), consistent with the relatively low magnitude of $k''_{O_3,app,PG}$. Ninety-nine percent PG loss was only achieved at an O$_3$ dose of 5 mg/L (104 μM). Measured losses of fast-reacting (i.e., $k''_{O_3,app} > 5 \times 10^4$ M^{-1} s^{-1}) antibacterial substrates during ozonation of Kloten-Opfikon wastewater were >99% at O$_3$ doses $\geq$3 mg/L (63 μM) (Figure 3a). TET was >99% transformed at an O$_3$ dose of 1.5 mg/L (31 μM) (Figure 3a), consistent with the high magnitude of $k''_{O_3,app,TET}$ at pH 7.7 (Table 4). Observed losses of SMX (Figure 3a) agree well with results reported for pilot-scale ozonation of Kloten-Opfikon wastewater at an O$_3$ dose of 1 mg/L (*18*). RX, AZ, AM, and LM were not included in these experiments because of analytical difficulties. Predicted losses for these four substrates were calculated for an applied O$_3$ dose of 1 mg/L (Figure 3a), as described in Text S5. The values calculated for RX and AZ (Figure 3a) agree very well with pilot-scale measurements under similar conditions (*18*).

Role of O$_3$ and •OH in Oxidation of Parent Molecules. Pollutant transformation during a real water ozonation process can be characterized by eq 3 (*34*):

$$\ln\left(\frac{[M]_\tau}{[M]_0}\right) = -k''_{O_3,app,M}\int_0^\tau[O_3]\,dt - k''_{•OH,app,M}\int_0^\tau[•OH]\,dt \tag{3}$$

where the two integral terms in eq 3 represent the O$_3$ and •OH exposures (*26*, *34*) governing transformation of substrate M over reaction time τ, where [•OH] = $f(t)$ and [O$_3$] = $g(t)$. $k''_{•OH,app,M}$ values measured for each antibacterial compound range from 2.9 to 8.5 × 10^9 M^{-1} s^{-1} at pH 7 (Table 4).

As illustrated in Figure 3b, the transformation efficiencies determined for each substrate in Kloten-Opfikon wastewater correlate well with the magnitude of $k''_{O_3,app,M}$. In contrast, there is no clear relation between transformation efficiency and $k''_{•OH,app,M}$ for these conditions (inset to Figure 3b). This indicates that [M]/[M]$_0$ is governed primarily by the O$_3$ oxidation term in eq 3. The •OH oxidation term becomes important only if the magnitude of the O$_3$ oxidation term is relatively small, as a consequence of low $k''_{O_3,app,M}$, low $\int_0^\tau[O_3]\,dt$, or high $\int_0^\tau[•OH]\,dt$.
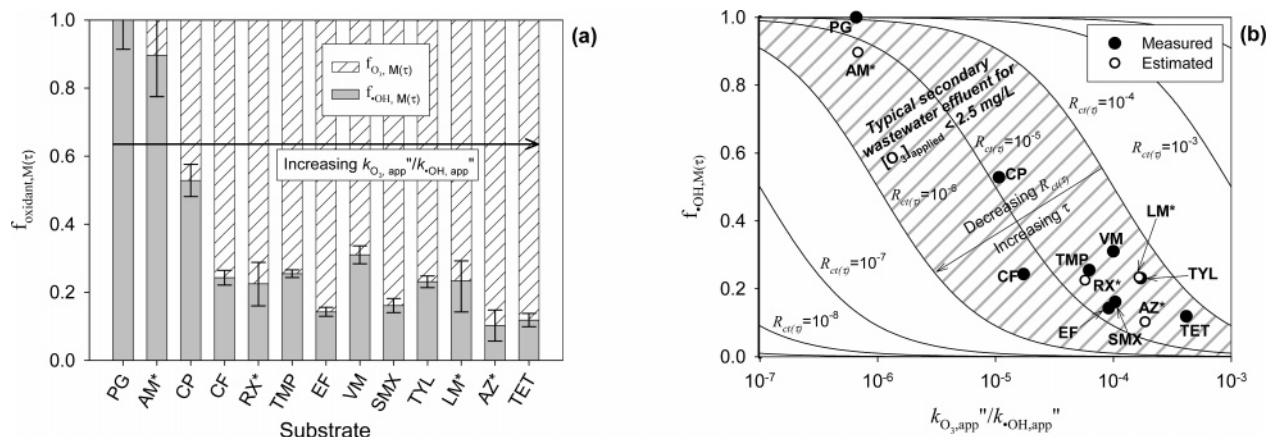
FIGURE 4. Importance of O_3 and $\bullet OH$ in transformation of substrates with $k''_{O_3,app} > 10^3 \text{ M}^{-1}\text{ s}^{-1}$ during ozonation of Kloten-Opfikon secondary effluent at 20 (± 0.5) °C, pH 7.7, [substrate]$_0$ = 1 μM, and [O_3]$_0$ = 21 μM (1 mg/L). (a) Calculated fractions of observed substrate transformation due to O_3 and $\bullet OH$. (b) Correlation of measured values of $f_{\bullet OH,M(\tau)}$ (obtained via eq 6) with values calculated via eq 4 for the range of $R_{ct(\tau)}$ values (25) expected for Kloten-Opfikon wastewater under these conditions. τ corresponds to reaction time after O_3 dosage. $R_{ct(\tau)}$ represents the cumulative ratio of $\bullet OH$ exposure to O_3 exposure for a pollutant molecule after reaction time, τ. The asterisks (*) indicate that estimates of % transformation and $f_{\bullet OH,M(\tau)}$ for RX, AZ, LM, and AM were calculated via procedures described in Text S5.

Contributions of O_3 and $\bullet OH$ to oxidation of ASMX were evaluated according to eq 4:

$$f_{\bullet OH,M(\tau)} = \frac{k''_{\bullet OH,app,M}\int_0^\tau [\bullet OH]\, dt}{k''_{O_3,app,M}\int_0^\tau [O_3]\, dt + k''_{\bullet OH,app,M}\int_0^\tau [\bullet OH]\, dt} =$$
$$\left(1 + \frac{k''_{O_3,app,M}}{k''_{\bullet OH,app,M}}\left(\frac{1}{\int_0^\tau [\bullet OH]\, dt / \int_0^\tau [O_3]\, dt}\right)\right)^{-1} \quad (4)$$

where $f_{\bullet OH,M(\tau)}$ represents the fraction of substrate oxidation due to $\bullet OH$ after reaction time, τ. $\int_0^\tau [O_3]\, dt$ was obtained by direct measurement of O_3 (via the indigo method (35)), and $\int_0^\tau [\bullet OH]\, dt$ was determined from the measured loss of the $\bullet OH$ probe p-chlorobenzoic acid (pCBA), which reacts rapidly with $\bullet OH$ and negligibly with O_3, according to eq 5 (34).

$$\ln\left(\frac{[p\text{CBA}]_\tau}{[p\text{CBA}]_0}\right) = -k''_{\bullet OH,app,p\text{CBA}}\int_0^\tau [\bullet OH]\, dt \quad (5)$$

These calculations indicated that ASMX was transformed exclusively by $\bullet OH$ (Figure S12).

Transformations of substrates with $k''_{O_3,app} > 10^3 \text{ M}^{-1}\text{ s}^{-1}$ were also characterized according to the relationships shown in eq 4. However, because $\int_0^\tau [O_3]\, dt$ could not be measured during the course of each substrate's transformation in Kloten-Opfikon wastewater, $f_{\bullet OH,M(\tau)}$ was actually calculated from eq 6 (18), which is obtained by substitution of eqs 3 and 5 into eq 4.

$$f_{\bullet OH,M(\tau)} = \frac{\dfrac{k''_{\bullet OH,app,M}}{k''_{\bullet OH,app,p\text{CBA}}}\ln\left(\dfrac{[p\text{CBA}]_\tau}{[p\text{CBA}]_0}\right)}{\ln\left(\dfrac{[M]_\tau}{[M]_0}\right)} \quad (6)$$

Although values obtained via eq 6 provide no information as to temporal variation of $\int_0^\tau [O_3]\, dt$ during ozonation, this expression can still provide reliable estimates of the absolute contributions of $\bullet OH$ and O_3 to bulk substrate oxidation. For example, $f_{\bullet OH,M(\tau)}$ values calculated by eq 6 for the antiepileptic drug carbamazepine (with $k''_{O_3,app} \sim 3 \times 10^5 \text{ M}^{-1}\text{ s}^{-1}$, $k''_{\bullet OH} = 8.8\ (\pm 1.2) \times 10^9 \text{ M}^{-1}\text{ s}^{-1}$ at pH 7 (17)) typically exhibit deviations of less than 10% from values determined by eq 4, using measurements of O_3 and $\bullet OH$ exposure actually taken within the first few hundred milliseconds after application of O_3 to various municipal wastewaters (Figure S14). $f_{\bullet OH,M(\tau)}$ values calculated by eq 6 are summarized in Figure 4a. According to eq 4 (from which eq 6 is derived), $f_{\bullet OH,M(\tau)}$ should be inversely related to the ratio $k''_{O_3,app,M}/k''_{\bullet OH,app,M}$, consistent with the general trend shown in Figure 4a.

Effects of Matrix Characteristics on Relative Importance of O_3 and $\bullet OH$ in Observed Substrate Transformation. As evident from eq 4, $f_{\bullet OH,M(\tau)}$ for a given substrate will also depend on the time-dependent ratio of $\int_0^\tau [\bullet OH]\, dt / \int_0^\tau [O_3]\, dt$, or $R_{ct(\tau)}$ (25, 33, 34, 36), during wastewater ozonation. $R_{ct(\tau)}$ is particularly sensitive to wastewater DOC concentrations, where higher DOC typically translates to higher $R_{ct(\tau)}$ values (25, 36). The solid lines shown in Figure 4b illustrate expected $f_{\bullet OH,M(\tau)}$ values (calculated from eq 4) as a function of $k''_{O_3,app,M}/k''_{\bullet OH,app,M}$, for a number of $R_{ct(\tau)}$ values. The shaded region shown in Figure 4b represents the apparent range of $R_{ct(\tau)}$ values previously observed (at O_3 doses varying from 1 to 2.5 mg/L for various municipal wastewaters during the time scales (<10 s) within which the bulk of fast-reacting substrate loss (i.e., >90%) is expected to occur (25, 33). In accordance with these expectations, the $f_{\bullet OH,M(\tau)}$ values obtained by eq 6 (for an applied O_3 dose of 1 mg/L) for each fast-reacting substrate included in the present investigation fall within this shaded region (Figure 4b). The relationships presented in Figure 4b suggest that $f_{\bullet OH,M(\tau)}$ for substrates with values of $k''_{O_3,app,M}/k''_{\bullet OH,app,M} < 10^{-6}$ will range from about 0.5 to 1 during ozonation of a typical wastewater. However, $f_{\bullet OH,M(\tau)}$ can be expected to vary between 0.1 and 0.9 for substrates with $k''_{O_3,app,M}/k''_{\bullet OH,app,M}$ ranging from 10^{-6} to 10^{-4}. In contrast, $f_{\bullet OH,M(\tau)}$ will generally be relatively small (<0.5) for substrates with $k''_{O_3,app,M}/k''_{\bullet OH,app,M} > 10^{-4}$.

Implications for Selective Oxidation during Wastewater Ozonation. Many of the antibacterial substrates included in this study are expected to be transformed predominantly via direct oxidation by O_3 during wastewater ozonation (Figure 4b). However, PG, CP, AM, and ASMX (each with $k''_{O_3,app,M}/k''_{\bullet OH,app,M} \leq 10^{-5}$ at circumneutral pH) will generally be transformed to a large extent by $\bullet OH$ during wastewater ozonation.

This may be undesirable in the case of AM, since $\bullet OH$ will likely react indiscriminately with many sites not associated with the AM molecule's antibacterial activity (Table 1 and Text S1). With respect to ASMX, however, $\bullet OH$ may be no less desirable as an oxidant than O_3, because O_3 appears to react only very slowly (if at all) with the biochemically essential p-sulfonylaniline target (Table 1, Table 4). Oxidation of PG

and CP by •OH may actually be more desirable than oxidation by O_3, since •OH reactions lead primarily to production of biochemically inactive (37) benzylpenilloic and benzylpenicilloic acids (29).

In the case of CF and EF, the relatively low ratios of $k''_{O_3,app,target}$ (i.e., $k''_{O_3,app,FLU}$) to $k''_{OH,app,M}$ (i.e., $<10^{-6}$, according to Figure 1b and Table 4) suggest that nonessential locations within each fluoroquinolone's structure may be oxidized to a significant extent by •OH and O_3 prior to reaction of O_3 with their essential quinolone target moieties. On the assumption that preoxidation of other locations within the parent fluoroquinolone structures (by O_3 or •OH) does not significantly reduce the reactivity of their target moieties toward O_3, full oxidation of the target moieties can likely still be accomplished by selecting an applied O_3 dose to achieve a sufficiently high $\int_0^\tau [O_3]\, dt$ value, which should be chosen on the basis of moiety-specific oxidation kinetics, as opposed to apparent substrate transformation kinetics.

Acknowledgments

Supporting Information Available

Text, figures, and tables addressing materials, experimental procedures, substrate reactive sites, and biochemical mechanisms of antibacterial activity. This material is available free of charge via the Internet at http://pubs.acs.org.

Literature Cited

(1) Hirsch, R.; Ternes, T. A.; Haberer, K.; Kratz, K.-L. Occurrence of antibiotics in the environment. *Sci. Total Environ.* **1999**, *225*, 109−118.

(2) Golet, E. M.; Xifra, I.; Siegrist, H.; Alder, A. C.; Giger, W. Environmental exposure assessment of fluoroquinolone antibacterial agents from sewage to soil. *Environ. Sci. Technol.* **2003**, *37*, 3243−3249.

(3) Miao, X.-S.; Bishay, F.; Chen, M.; Metcalfe, C. D. Occurrence of antimicrobials in the final effluents of wastewater treatment plants in Canada. *Environ. Sci. Technol.* **2004**, *38*, 3542−3550.

(4) Göbel, A.; Thomsen, A.; McArdell, C. S.; Joss, A.; Giger, W. Occurrence and sorption behavior of sulfonamides, macrolides, and trimethoprim in activated sludge treatment. *Environ. Sci. Technol.* **2005**, *39*, 3981−3989.

(5) Lindberg, R. H.; Wennberg, P.; Johansson, M. I.; Tysklind, M.; Andersson, B. A. V. Screening of human antibiotic substances and determination of weekly mass flows in five sewage treatment plants in Sweden. *Environ. Sci. Technol.* **2005**, *39*, 3421−3429.

(6) Kim, S.; Eichorn, P.; Jensen, J. N.; Weber, A. S.; Aga, D. S. Removal of antibiotics in wastewater: effect of hydraulic and solid retention times on the fate of tetracycline in the activated sludge process. *Environ. Sci. Technol.* **2005**, *39*, 5816−5823.

(7) Brain, R. A.; Johnson, D. J.; Richards, S. M.; Hanson, M. L.; Sanderson, H.; Lam, M. W.; Young, C.; Mabury, S. A.; Sibley, P. K.; Solomon, K. R. Microcosm evaluation of the effects of an eight pharmaceutical mixture to the aquatic macrophytes *Lemna gibba* and *Myriophyllum sibiricum. Aquat. Toxicol.* **2004**, *70*, 23−40.

(8) Wilson, C. J.; Brain, R. A.; Sanderson, H.; Johnson, D. J.; Bestari, K. T.; Sibley, P. K.; Solomon, K. R. Structural and functional responses of plankton to a mixture of four tetracyclines in aquatic microcosms. *Environ. Sci. Technol.* **2004**, *38*, 6430−6439.

(9) Wilson, B. A.; Smith, V. H.; Denoyelles, F.; Larive, C. K. Effects of three pharmaceutical and personal care products on natural freshwater algal assemblages. *Environ. Sci. Technol.* **2003**, *37*, 1713−1719.

(10) *Antibiotics in Laboratory Medicine*, 4th ed.; Lorian, V., Ed.; Williams and Wilkins: Baltimore, MD, 1996.

(11) Baquero, F. Low-level antibacterial resistance: a gateway to clinical resistance. *Drug Resist. Updates* **2001**, *4*, 93−105.

(12) Drlica, K. The mutant selection window and antimicrobial resistance. *J. Antimicrob. Chemother.* **2003**, *52*, 11−17.

(13) Paraskeva, P.; Graham, N. J. D. Ozonation of municipal wastewater effluents. *Water Environ. Res.* **2002**, *74*, 569−581.

(14) Beltran, F. J.; Garcia-Araya, J. F.; Alvarez, P. M. Integration of continuous biological and chemical (ozone) treatment of domestic wastewater: 2. Ozonation followed by biological oxidation. *J. Chem. Technol. Biotechnol.* **1999**, *74*, 884−890.

(15) Gehr, R.; Wagner, M.; Veerasubramanian, P.; Payment, P. Disinfection efficiency of peracetic acid, UV and ozone after enhanced primary treatment of municipal wastewater. *Water Res.* **2003**, *37*, 4573−4586.

(16) Adams, C.; Wang, Y.; Loftin, K.; Meyer, M. Removal of antibiotics from surface and distilled water in conventional water treatment processes. *J. Environ. Eng.* **2002**, *128*, 253−260.

(17) Huber, M. M.; Canonica, S.; Park, G.-Y.; von Gunten, U. Oxidation of pharmaceuticals during ozonation and advanced oxidation processes. *Environ. Sci. Technol.* **2003**, *37*, 1016−1024.

(18) Huber, M. M.; Göbel, A.; Joss, A.; Hermann, N.; Löffler, D.; McArdell, C. S.; Ried, A.; Siegrist, H.; Ternes, T. A.; von Gunten, U. Oxidation of pharmaceuticals during ozonation of municipal wastewater effluents: a pilot study. *Environ. Sci. Technol.* **2005**, *39*, 4290−4299.

(19) Ternes, T. A.; Stüber, J.; Herrmann, N.; McDowell, D.; Ried, A.; Kampmann, M.; Teiser, B. Ozonation: a tool for removal of pharmaceuticals, contrast media and musk fragrances from wastewater? *Water Res.* **2003**, *37*, 1976−1982.

(20) Huber, M. M.; Ternes, T.; von Gunten, U. Removal of estrogenic activity and formation of oxidation products during ozonation of 17α-ethinylestradiol. *Environ. Sci. Technol.* **2004**, *38*, 5177−5186.

(21) Hoigné, J.; Bader, H. Rate constants of reactions of ozone with organic and inorganic compounds in water−II: Dissociating organic compounds. *Water Res.* **1983**, *17*, 185−194.

(22) Pryor, W. A.; Giamalva, D. H.; Church, D. F. Kinetics of ozonation. 2. Amino acids and model compounds in water and comparisons to rates in nonpolar solvents. *J. Am. Chem. Soc.* **1984**, *106*, 7094−7100.

(23) Qiang, Z.; Adams, C.; Surampalli, R. Determination of ozonation rate constants for lincomycin and spectinomycin. *Ozone: Sci. Eng.* **2004**, *26*, 525−537.

(24) Mvula, E.; von Sonntag, C. Ozonolysis of phenols in aqueous solution. *Org. Biomol. Chem.* **2003**, *1*, 1749−1756.

(25) Buffle, M.-O.; Schumacher, J.; Meylan, S.; Jekel, M.; von Gunten, U. Ozonation and advanced oxidation of wastewater: Effect of O_3 dose, pH, DOC and HO•-scavengers on ozone decomposition and HO• generation. *Ozone: Sci. Eng.* **2006**, submitted.

(26) von Gunten, U. Ozonation of drinking water: Part I. Oxidation kinetics and product formation. *Water Res.* **2003**, *37*, 1443−1467.

(27) Hoigné, J.; Bader, H. Rate constants of reactions of ozone with organic and inorganic compounds in water−I: Non-dissociating organic compounds. *Water Res.* **1983**, *17*, 173−183.

(28) Leitzke, A.; Reisz, E.; Flyunt, R.; von Sonntag, C. The reactions of ozone with cinnamic acids: formation and decay of 2-hydroperoxy-2-hydroxyacetic acid. *J. Chem. Soc., Perkin Trans. 2* **2001**, 793−797.

(29) Phillips, G. O.; Power, D. M.; Robinson, C. Chemical changes following γ-irradiation of benzylpenicillin in aqueous solution. *J. Chem. Soc., Perkin Trans. 2* **1973**, 575−582.

(30) Neta, P.; Dorfman, L. M. Pulse radiolysis studies. XIII. Rate constants for the reaction of hydroxyl radicals with aromatic compounds in aqueous solutions. *Adv. Chem.* **1968**, *81*, 222−230.

(31) Dowideit, P.; von Sonntag, C. Reaction of ozone with ethene and its methyl- and chlorine-substituted derivatives in aqueous solution. *Environ. Sci. Technol.* **1998**, *32*, 1112−1119.

(32) Onstad, G. D.; Strauch, S.; Meriluoto, J.; Codd, G.; von Gunten, U. Selective oxidation of key functional groups in cyanotoxins during drinking water ozonation. *Environ. Sci. Technol.* **2006**, submitted.

(33) Buffle, M.-O.; Schumacher, J.; Salhi, E.; Jekel, M.; von Gunten, U. Measurement of the initial phase of ozone decomposition in water and wastewater by means of a continuous quench flow system: Application to disinfection and pharmaceutical oxidation. *Water Res.* **2006**, submitted.

(34) Elovitz, M. S.; von Gunten, U. Hydroxyl radical/ozone ratios during ozonation processes. I. The R_{ct} concept. *Ozone: Sci. Eng.* **1999**, *21*, 239−260.

(35) Bader, H.; Hoigné, J. Determination of ozone in water by the indigo method. *Water Res.* **1981**, *15*, 449−456.

(36) Elovitz, M. S.; von Gunten, U.; Kaiser, H. P. Hydroxyl radical/ozone ratios during ozonation processes. II. The effect of temperature, pH, alkalinity, and DOM properties. *Ozone: Sci. Eng.* **2000**, *22*, 123−150.

(37) Walsh, C. *Antibiotics: Actions, Origins, Resistance*; ASM Press: Washington, DC, 2003.